IEEE Access
Multidisciplinary ⋮ Rapid Review ⋮ Open Access Journal

Received 2 June 2022, accepted 21 July 2022, date of publication 5 August 2022, date of current version 22 August 2022.

*Digital Object Identifier 10.1109/ACCESS.2022.3196687*

RESEARCH ARTICLE

# Wideband and High Gain Array Antenna for 5G Smart Phone Applications Using Frequency Selective Surface

**RAZA ULLAH[1], SADIQ ULLAH[1], (Senior Member, IEEE), RIZWAN ULLAH[1], IFTIKHAR UD DIN[1], BABAR KAMAL[2], MUHAMMAD ALTAF HUSSAIN KHAN[1], AND LADISLAU MATEKOVITS[3,4,5], (Senior Member, IEEE)**

[1]Telecommunication Engineering Department, University of Engineering & Technology Mardan, Mardan, Khyber Pakhtunkhwa 23200, Pakistan
[2]Center of Intelligent Acoustics and Immersive Communications, Northwestern Polytechnical University, Xi'an 710072, China
[3]Department of Electronics and Telecommunications, Politecnico di Torino, 10129 Turin, Italy
[4]Istituto di Elettronica e di Ingegneria dell'Informazione e delle Telecomunicazioni, National Research Council of Italy, 10129 Turin, Italy
[5]Department of Measurements and Optical Electronics, Politehnica University Timisoara, 300006 Timisoara, Romania

Corresponding authors: Sadiq Ullah (sadiqullah@uetmardan.edu.pk) and Ladislau Matekovits (ladislau.matekovits@polito.it)

This work was supported in part by the University of Engineering and Technology Mardan.

**ABSTRACT** This work presents an eight element array antenna with single layer frequency selective surface (FSS) to obtain high gain. The eight elements are fed by single port. The FSS consists of $14 \times 6$ unit cells with one unit cell size is $5 \times 5$ mm$^2$ having wideband behavior. The antenna uses Rogers RT Duroid 5880 substrate and giving very wide bandwidth from 20 GHz to 65 GHz, covering millimeter wave 5G bands (including 28 GHz, 38 GHz and 60 GHz). The designed FSS is showing stop band transmission characteristics below $-10$ dB threshold from 25 GHz to 42 GHz and 59 GHz to 61 GHz. The eight element antenna integrated with the FSS reflector, which results an improvement in the gain level from 12 dB to 15 dB at 28 GHz, from 10 dB to 12 dB at 38 GHz, and from 9.5 to 11 dB at 60 GHz. The dimensions of the antenna are $65 \times 27 \times 0.857$ mm$^3$. The proposed antenna shows stable gain and directional radiation patterns. The simulation findings are experimentally confirmed, by testing the fabricated prototypes of the proposed antenna system.

**INDEX TERMS** 5G, array antenna, FSS, mobile communication.

## I. INTRODUCTION

With the rapid increase of mobile communication users over the last decade, the need for higher channel capacity and wider bandwidth have been exponentially increased. In order to meet these increasing demand, fifth generation (5G) is one of the promising technology, which can provide higher data rates up to 20 Gbps, and very low latency of 1 ms [1], [2], improved reliability, connectivity of millions of devices with low power consumption and support for modern technologies such as autonomous cars, smart cities and virtual reality [3]. As many of the nations that are regarded leaders in 5G technology, development, and deployment (such as United States, Korea, Japan, United Kingdom, Canada, China, and the European Union) are employing millimetre wave band for 5G communication [4]. As due to scarcity and congestion in sub-6 GHz frequency spectrum, millimeter wave spectrum is the potential spectrums for 5G mobile applications [5]. Moreover, the absolute bandwidth provide by millimeter wave frequencies is much larger than the the bandwidth provided by sub-6 GHz [6]. However, in millimeter wave bands there are some key factors that should be considered. As at higher frequencies bands free space path loss, user hand effects and shadowing effect are severe during the propagation [7]. Therefore, in order to compensate these losses, the gain of the transmitter and receiver antennas needs to be increased, without using additional power [8].

The associate editor coordinating the review of this manuscript and approving it for publication was Eyuphan Bulut.

In recent literature, several types of antennas and techniques have been proposed to solve the problems of path loss, user hand effects and shadowing effect. In [9] and [10] a planer waveguides based, array antennas with high gain and wide band are reported. Three identical sub-arrays are positioned along the upper portion of the device with the beam steering capabilities, consisting of rectangular patches in [11] and capacitive linked patches is reported in [12]. In [13], [14] phased arrays working in the millimeter wave frequencies have been used in the mobile devices, despite the fact that their all of the constructions are three-dimensional, integration is tough. Planar phased array antennas, including patch, vivaldi, quasi-Yagi, and slot antennas, were proposed in different forms in [15]–[17]. In [12], a planar eight identical elements array for 5G applications is reported. Moreover, in diverse user settings, a circularly polarized phased array in the portable device was investigated [18]. In [19] proposes a unique design combining a low-frequency PIFA antenna with millimeter wave end fire antenna array. The millimeter wave antenna array has a wide bandwidth of more than 9 GHz, and a gain of 9.5 dBi, with coverage efficiencies of 85 % and 55 % for gain of 0 dB and 4 dBi, accordingly. However, in the above literatures, most of the antenna designs are showing limitations in respect of high gain, fabrication complexity, and operational bandwidth. Our proposed antenna has high gain, wide bandwidth, simple fabrication, and covering all the candidate frequencies considered for 5G millimeter wave communications.

In this work, by applying parametric analysis from designs A- F in Fig.1, finally the optimized single element is obtained which shows wide band characteristic covering range from 20 GHz to 65 GHz. This covers 28 GHz frequency band including 38 GHz and 60 GHz bands, these all are considered candidate frequencies for the 5G mobile applications [23]–[28]. The antenna with one element is showing good characteristics in terms of radiation patterns but having limitation of low gain values (i.e., 3 dB, 4 dB, 4 dB), at the aforementioned frequencies of 28 GHz, 38 GHz, and 60 GHz, respectively. In order to compensate high gain requirement, the optimized one element antenna is converted to two, four and finally to eight element antenna. The final design having eight elements showing maximum gain levels of 12 dB, 10 dB, and 9.5 dB. To further increase the gain, unit cell metamaterial is designed. Parametric analysis was carried out on metamaterial unit cell to get the optimized one in order to cover the wide range of targeted frequencies. The final optimized metamaterial unit cell is covering all aimed bands and showing band stop behavior at the targeted bands. In order to get further improvement in gain, single layer frequency selective surface is made having 14 × 6 unit cells. The FSS reflector is introduced at back side of the eight elements antenna at 5 mm space. It is observed good improvement in gain values that are 15 dB at 28 GHz, 12 dB at 38 GHz, and 11 dB at 60 GHz. The proposed designs of antenna and FSS were fabricated. The simulated and measured results show good agreement. This work was compared to related work which shows obvious superiority in terms of gain, wide bandwidth and operational frequencies.

**TABLE 1. Dimensions of the single element antenna.**

| Parameter | $h_1$ | $h_2$ | $h_3$ | $h_4$ | $h_5$ | $h_6$ | $h_o$ |
|---|---|---|---|---|---|---|---|
| Value (mm) | 2.3 | 0.4 | 2.625 | 0.4 | 2.325 | 3.2 | 0.5 |
| Parameter | $b_1$ | $b_2$ | $b_3$ | $b_4$ | $b_5$ | $b_6$ | $h_g$ |
| Value (mm) | 0.65 | 1.075 | 0.4 | 0.325 | 0.4 | 0.4 | 1.8 |

The remaining part of the paper is structured as follows: section 2 discusses design and optimization of the single element and eight elements antenna. Section 3 discussed the design of unit cell and its FSS array. Section 4 presented the comparison between simulated and fabricated design. The comparison of the proposed design with related work is carried out in section 5. The last section 6, presents conclusion of the proposed work.

## II. DESIGN AND OPTIMIZATION

The steps followed for the design of single element antenna have been discussed in detail in this section. The single element is replaced by the multi elements designs as per the required needs for the 5G applications. Rogers 5880 has been used as a substrate with thickness 0.787 mm, relative permittivity of 2.2, and loss tangent of 0.0009. The upper arm and lower with the truncated ground are made of copper conductor.

### A. OPTIMIZATION OF THE SINGLE ELEMENT ANTENNA

The evolution of the initial to final design is achieved in six stages as shown in Fig. 1. The initial design type-A has only one main arm on the front and similarly on the back side. The length of the arm is taken half of wavelength at 38 GHz. The type-A shows no behavior for being acting as an antenna at any 5G frequency bands. A small upper arm is made with addition of a stub in type-B. The type-B covers dual frequency ranges from 22 GHz to 29 GHz and from 33 GHz to 40 GHz. In order to cover 60 GHz, the type-C is introduced with addition of lower arm due to which covering range from 47 GHz to 64 GHz is achieved. Type-C covers all bands but showing bandwidth limitation at 38 GHz. The bandwidth is enhanced by introducing left most vertical arm in type-D design with absence of stub. The bandwidth is increased but shows instability in behavior due to removing of stub. In type-E, the upper arm is removed in order to verify its significance. It can be seen that type-E covers only higher frequency bands. Finally, the optimized single element antenna type-F is designed which covers wide bandwidth ranging from 20 GHz to 65 GHz. The type-F antenna covers 5G candidate frequencies which are 28 GHz including 38 GHz and 60 GHz. The optimized final version type-F is obtained by varying the relative positions, sizes including lengths and widths of the main arm, upper/lower arms, vertical arm, stub and height of the ground. The height of the

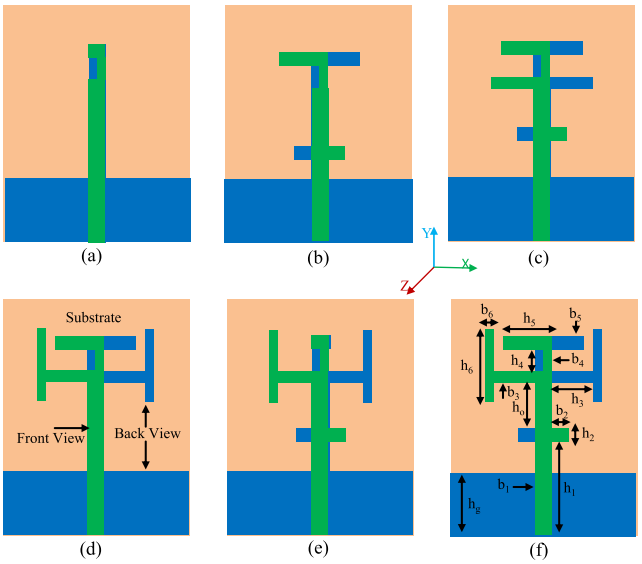


**FIGURE 1.** Evolution of single element antenna (a) Single arm (b) Upper arm (c) Upper and Lower arms (d) Addition of vertical arm (e) Removing Upper arm and (f) Optimized single element antenna.

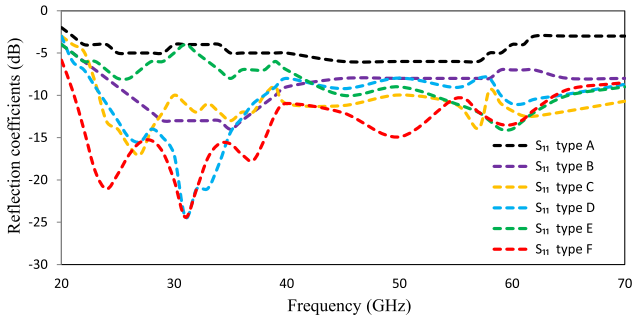


**FIGURE 2.** Comparison of reflection coefficients of single element designs with the optimized single element design.

**TABLE 2.** Dimensions of the eight element antenna.

| Parameter | $L_1$ | $L_2$ | $L_3$ | $L_4$ | $L_5$ | $L_6$ | $W_1$ | $W_o$ |
|---|---|---|---|---|---|---|---|---|
| Value (mm) | 7 | 30 | 4.02 | 15 | 3.383 | 7.5 | 1.33 | 0.25 |

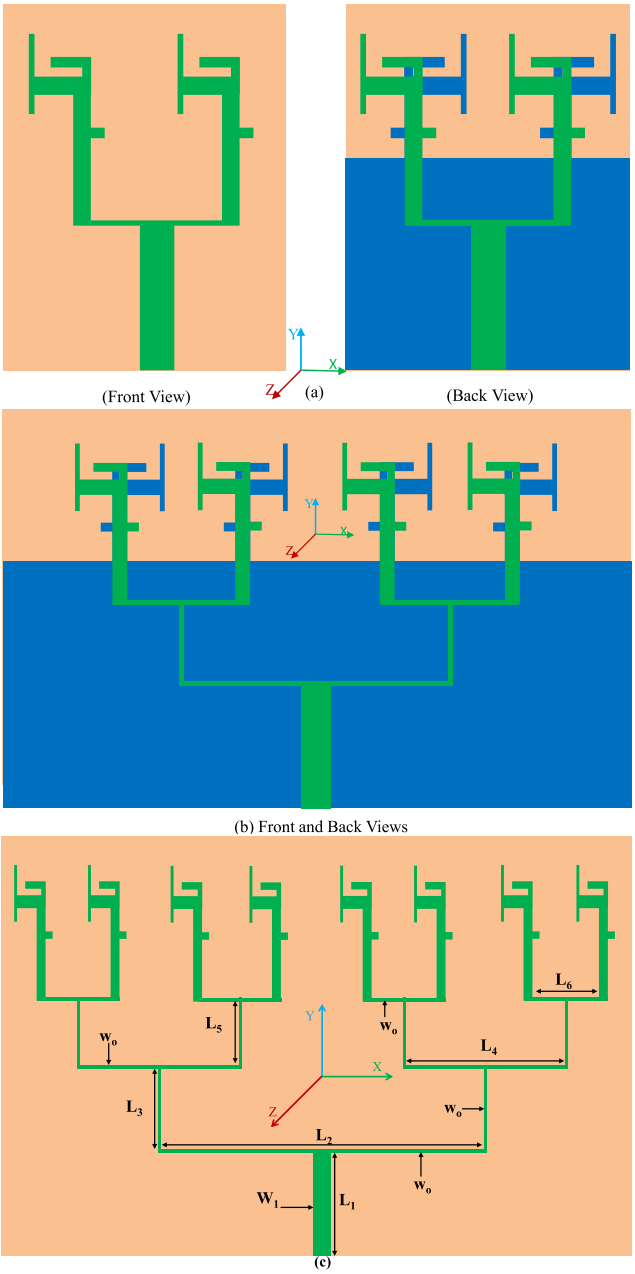


**FIGURE 3.** Geometries of the multi elements designs (a) Two elements antenna (b) Four elements antenna and (c) Eight elements antenna.

ground plane plays in important role in obtaining the optimized results due to its influence on the radiation characteristics of the antenna. All these parameters play an important role in the behavior of the antenna. The optimized parameters of the single element type-F are shown in Table 1. The proposed single element design is showing good characteristics like light weight, wide bandwidth, easy to fabricate and stable radiation patterns. Fig. 2 represents the reflection coefficients of all the six designs (type-A to type-F). These results are obtained by using CST microwave studio in the time domain.

### *B. OPTIMIZATION OF THE MULTI ELEMENT DESIGN*

The antenna with one element is showing good characteristics in terms of radiation patterns but having limitation of low gain values. Therefore, single element type-F design is converted to two, four and eight elements for compensating the need of high gain required for 5G applications as indicated in Fig. 3. To get broadside radiation pattern, 7.5 mm spacing is chosen between the inter-elements of the individual elements. The taper lines feeding network is provided to the multi elements designs. The end feeder is selected 50 Ω while all other taken 100 Ω. The widths and lengths of feeding lines have been selected according to the equations [29].

$$W_1 = \left(\frac{277}{Z_o\sqrt{\epsilon_r}} - 2\right)h \tag{1}$$

**TABLE 3.** Simulated radiation characteristics of the proposed antennas.

| (a) 1– Element | | | | | | (c) 4– Elements | | | | | |
|---|---|---|---|---|---|---|---|---|---|---|---|
| f (GHz) | Planes | MLM (dB) | MLD (deg) | HPBW (deg) | SLL (dB) | f (GHz) | Planes | MLM (dB) | MLD (deg) | HPBW (deg) | SLL (dB) |
| 28 | E | 4.33 | 95 | 171.9 | 0 | 28 | E | 9.38 | 91 | 121.5 | 0 |
| | H | 2.4 | 3 | 78.2 | –2.1 | | H | 4.9 | 2 | 20.7 | –1.3 |
| 38 | E | 5.88 | 88 | 108.4 | –7 | 38 | E | 6.89 | 87 | 85 | –2.7 |
| | H | 0.434 | 6 | 59.7 | –2.2 | | H | 7.51 | –8 | 15.5 | –2.6 |
| 60 | E | 4.75 | 87 | 160 | 0 | 60 | E | 7.99 | 87 | 45.9 | –6 |
| | H | 4.22 | 5 | 54 | –3.4 | | H | 7.19 | –4 | 35 | –2.8 |
| (b) 2– Elements | | | | | | (d) 8–Elements | | | | | |
| f (GHz) | Planes | MLM (dB) | MLD (deg) | HPBW (deg) | SLL (dB) | f (GHz) | Planes | MLM (dB) | MLD (deg) | HPBW (deg) | SLL (dB) |
| 28 | E | 6.55 | 93 | 149.3 | –3 | 28 | E | 13.5 | 91 | 45.5 | –5.2 |
| | H | 4.41 | 8 | 44.5 | –2.6 | | H | 8.2 | 2 | 9 | –4.9 |
| 38 | E | 7.85 | 86 | 97.6 | –3.1 | 38 | E | 11.3 | 93 | 52.5 | –3.8 |
| | H | 4.86 | –4 | 39 | –3.6 | | H | 7.33 | 1 | 10.6 | –1.9 |
| 60 | E | 7.6 | 88 | 90 | –4.8 | 60 | E | 9.5 | 95 | 37.5 | –1.8 |
| | H | 3.53 | –7 | 49.7 | –1.1 | | H | 4.82 | 4 | 26.5 | –0.9 |

$$W_o = (\frac{277}{Z_o\sqrt{\epsilon_r}} - 2)h \tag{2}$$

$$L_4 = \frac{L_2}{2} \text{ and } L_6 = \frac{L_2}{4} \tag{3}$$

$W_1$ represents width of end feeder line when $Z_o$ is 50 Ω. $W_o$ represents width of all other feed lines when $Z_o$ is 100 Ω. The main feeder of 50 ohm is further divided into equal feeders of 100 ohm in order to provide equivalent excitation signals to all elements of 50 ohm as these feeder lines are in parallel combination. $\epsilon_r$ represents relative permittivity and h shows height of the substrate. $L_2$, $L_4$ and $L_6$ are the horizontal lengths of the feed lines. The parameters of the feed lines network provided to eight element antenna are shown in Table 2. The simulated $S_{11}$, gain vs. frequency plots and the radiation patterns of the single and multi-element antennas are shown in Fig. 4, Fig. 5, and Fig. 6, respectively. A negligible variation observed in impedance ($S_{11} < -10$ dB) between the single and multi-elements designs as displayed in Fig. 4. The gain values are significantly increased by increasing elements from single to eight elements. Fig. 6 shows the comparison of radiation pattern in the two principal planes, that is, E-plane ($\phi = 90°$) and H-plane ($\phi = 0°$) which shows gain is increasing in parallel with the increasing number of elements in the array design. For measuring the mutual coupling between neighboring elements, the eight elements are fed by separate ports instead of single feed line as indicated in Fig. 7. It is important to mention that there is very minimal mutual coupling between elements because of proper selection of spacing between the adjacent elements. The inter-element spacing is 7.5 mm which is λ/2 distance at 20 GHz. The spacing taken at lowest frequency due to fact that mutual coupling is high at lower distance. Lower frequency required greater distance between elements as compared to higher frequency. Therefore, the lower frequency is chosen a reference frequency for calculating

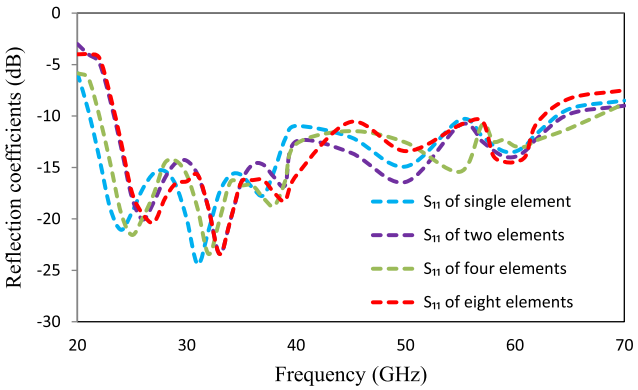


**FIGURE 4.** Comparison of reflection coefficients ($S_{11}$) of multi element designs.

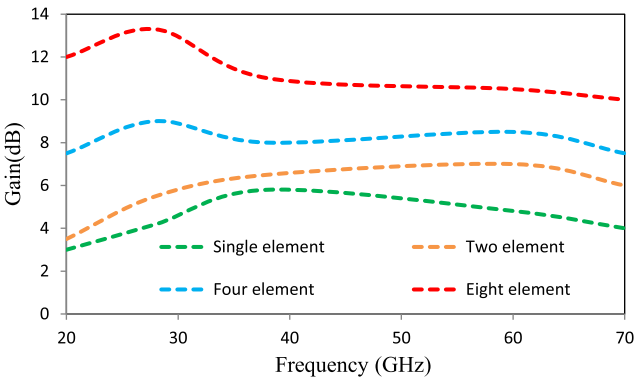


**FIGURE 5.** Comparison of Gain verses frequency of multi element designs.

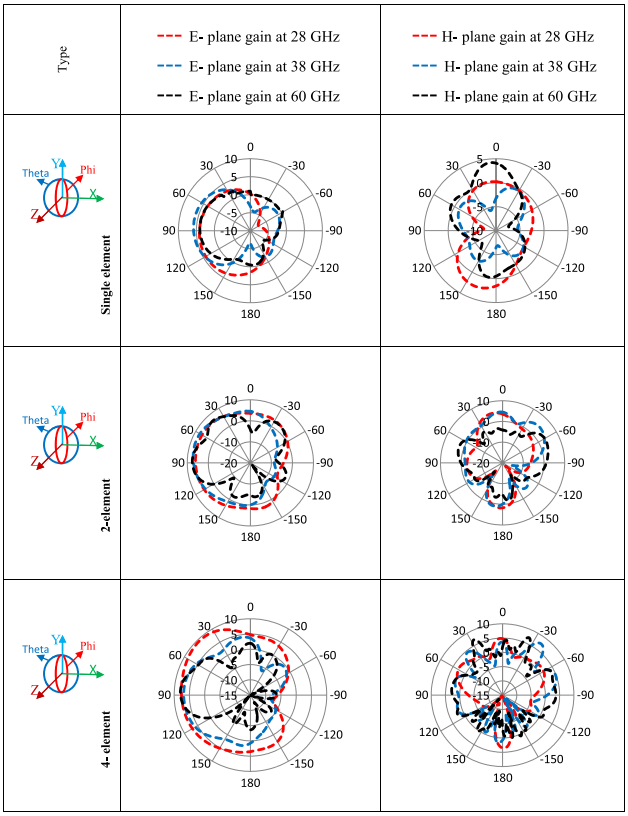


**FIGURE 6.** Comparison of radiation patterns in E and H planes at 28 GHz, 38 GHz and 60 GHz.

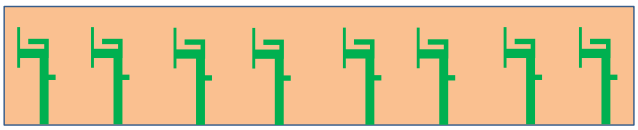

**FIGURE 7.** Eight elements are fed by separate ports for measuring mutual coupling between elements.

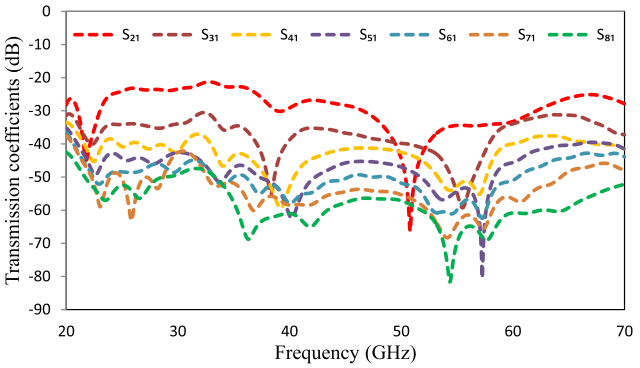


**FIGURE 8.** Transmission coefficients of eight element antenna.

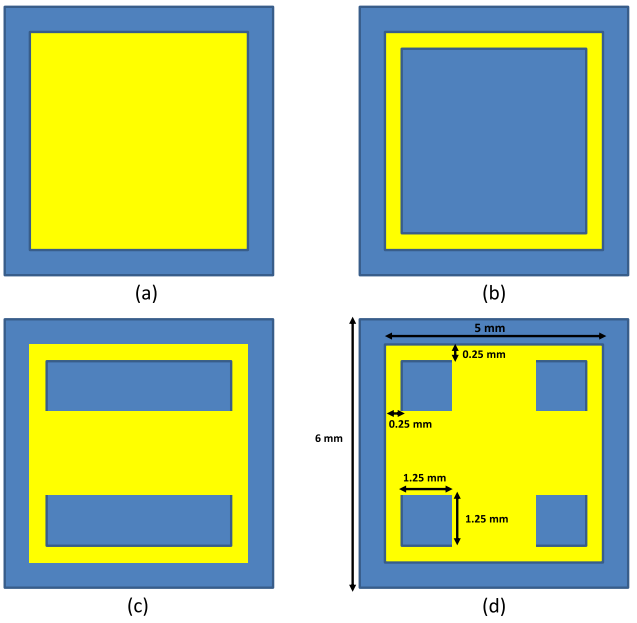


**FIGURE 9.** Optimization of the unit cell (a) Square patch (b) Square shape strip (c) Slots in the square patch (d) Optimized unit cell.

inter-elements spacing without mutual coupling. Fig. 8 shows mutual coupling between elements. The details of the simulated side lobe level (SLL) along with Main lobe Magnitude (MLM) including its direction (MLD) and Half Power Beam-width (HPBW) are presented in Table 3. It is noticeable that beam scanning along the main lobe direction occurs in the multiple elements design, compare to the single element design. It is obvious that gain is inversely to HPBW as the gain is increasing HPBW is decreasing simultaneously [29].

## III. DESIGN OF UNIT CELL FOR FSS CONFIGURATION

Frequency Selective Surface (FSS) are repeated periodic structures with one or two dimensions. FSS has unit cells which are aligned in periodic form. FSS structures have the capability to reflect, absorb or transmit the electromagnetic radiations depending on the design [20]–[22]. Rogers 5880 substrate with thickness 0.787 mm has been used for designing unit cell with dimension $5 \times 5$ mm$^2$. The simulations of the unit cells have been carried out in CST for obtaining the wide bandwidth covering all the targeted bands. The final version of unit cell is achieved with the result of evolution from Fig. 9 (a) to (d) for the aimed bands. The unit cell A with square patch achieves dual band operation which can stop band at 38 GHz with bandwidth 13 GHz from 30 GHz to 43 GHz and also shows stop band behavior at 60 GHz from 56.5 GHz to 60.3 GHz but limitation of covering of 28 GHz. Unit cell B with square shape strip is showing stop band characteristics at only 60 GHz with bandwidth of 0.7 GHz from 60 GHz to 60.7 GHz at $S_{21} < -10$ dB. In order to cover all the aimed bands, design of unit cell C is introduced which also shows limited operational behavior covering only lower bands, 28 GHz and 38 GHz with bandwidth of 20 GHz from 23 GHz to 43 GHz. The optimized final version unit cell D is designed which shows stop characteristics with improved $S_{21} < -10$ at the entire targeted bands. It covers from 25.5 GHz to 42 GHz with bandwidth of 16.5 GHz, and 59.6 GHz to 61 GHz with bandwidth of 1.4 GHz. The proposed unit cell has square shape with

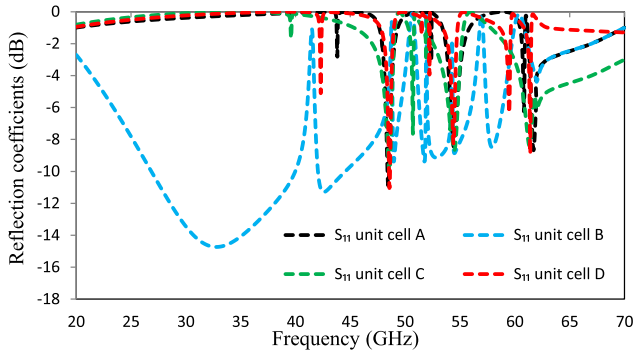


**FIGURE 10.** Comparison of reflection coefficients of the different unit cells with the optimized unit cell.

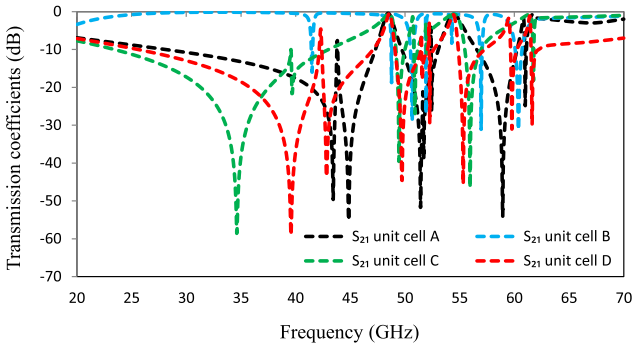


**FIGURE 11.** Comparison of transmission coefficients of the different unit cells with the optimized unit cell.

four square slots at the corners. The optimized version Fig. 9 (d) shows good performance for the targeted frequencies. The comparison of the reflection and transmission coefficients of all the unit cells are shown in Fig. 10, Fig.11, respectively.

### A. EIGHT ELEMENT ANTENNA WITH FSS ARRAY REFLECTOR

In order to achieve high gain values, the FSS array of 14 × 6 unit cells is introduced with optimized space of 5 mm at back face of the eight elements antenna design are displayed in Fig. 12. The integrated size of antenna with FSS reflector is slightly changed which is 66.75 × 28.75 × 6.679 $mm^3$. The proposed integrated antenna size is deployable in the mobile phones as normal mobile phones like Vivo Y53s has size of 164 × 75.46 × 8.38 $mm^3$. The gains enhancement achieved of 3 dB, 2 dB and 1.5 dB at 28 GHz, 38 GHz, 60 GHz, respectively. Comparison of gain without and with FSS is represented in Fig. 13. It is obviously observed that gains enhanced at the targeted frequencies without notable changes in the overall characteristics of the antenna. A detailed parametric study was carried out for obtaining the optimized space of 5 mm between antenna and FSS.

The proposed eight elements antenna with using FSS shows highest gain relatively to the rest of antennas designs

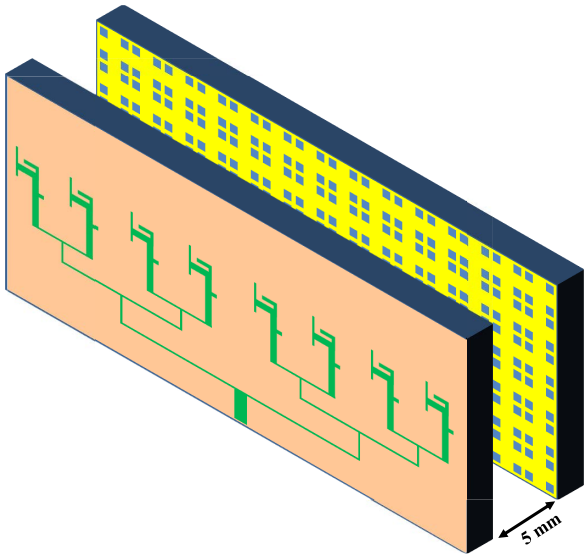


**FIGURE 12.** Eight element antenna with FSS of 14 × 6 unit cells.

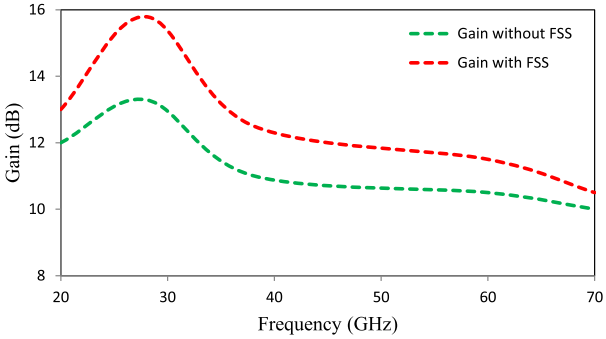


**FIGURE 13.** Comparison of gain without and with FSS of eight element antenna.

and is considered candidate antenna for 5G communications. This antenna is fabricated and the simulated results precisely compared and validated in the measurement facility.

## IV. RESULT DISCUSSION OF THE FABRICATED EIGHT ELEMENT ANTENNA

The eight elements array design is fabricated as given in Fig. 14. The simulated results including return loss, gain, radiation pattern, and efficiency are validated in the measurement facility. The comparison of simulated verses measured reflection coefficient ($S_{11}$) is given in Fig. 15 which are in close agreement.

The simulated and measured radiation patterns at 28 GHz, 38 GHz and 60 GHz in the two principal planes, E-plane (XZ @ $\phi = 90°$) and H-plane (YZ @ $\phi = 0°$) are compared in Fig. 16. This comparison shows closed agreement between the simulated and measured results of the radiation patterns. The direction of the main beam is oriented along $\theta = 0°$ and 180° as clearly observed from results. Also strong radiations are observed at other angles in this plane.

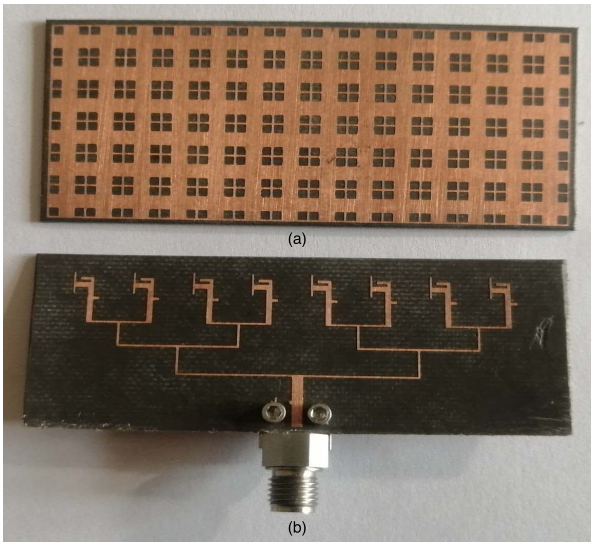


**FIGURE 14.** Photograph of the prototype: (a) FSS design (b) Eight elements antenna design.

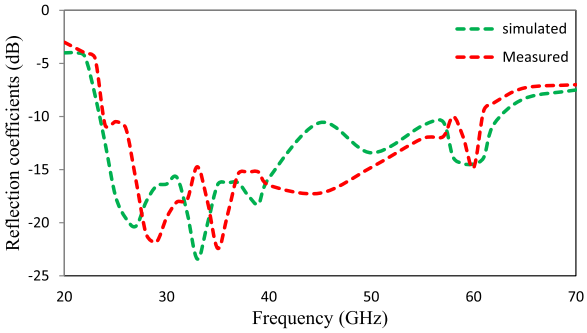


**FIGURE 15.** Comparison of simulated and measured reflection coefficients.

Fig. 17 shows comparison of simulated and measured gain plots as function of frequency. The measured gains values at the targeted frequencies are 15 dB at 28 GHz, 12 dB at 38 GHz and 11 dB at 60 GHz. The proposed array antenna design shows stable gain characteristics. Therefore, it can be considered for 5G communications due to its high gain capability.

To analyze the internal operating behavior of the proposed design at 28 GHz, 38 GHz and 60 GHz, the surface currents are illustrated in Fig. 18. It is observed that the currents at 28 GHz are concentrated at the center of the upper arm. At 38 GHz, currents are resided at the edges of the upper part while currents are concentrated at the lower arm at 60 GHz. It means that upper arm is effective at 28 GHz and 38 GHz while lower arm is responsible for 60 GHz.

Due to properly matched design, the simulated and measured radiation efficiency shows good agreement as illustrated in Fig. 19. The radiation efficiency of the proposed design at the aforementioned frequencies is above than acceptable value.

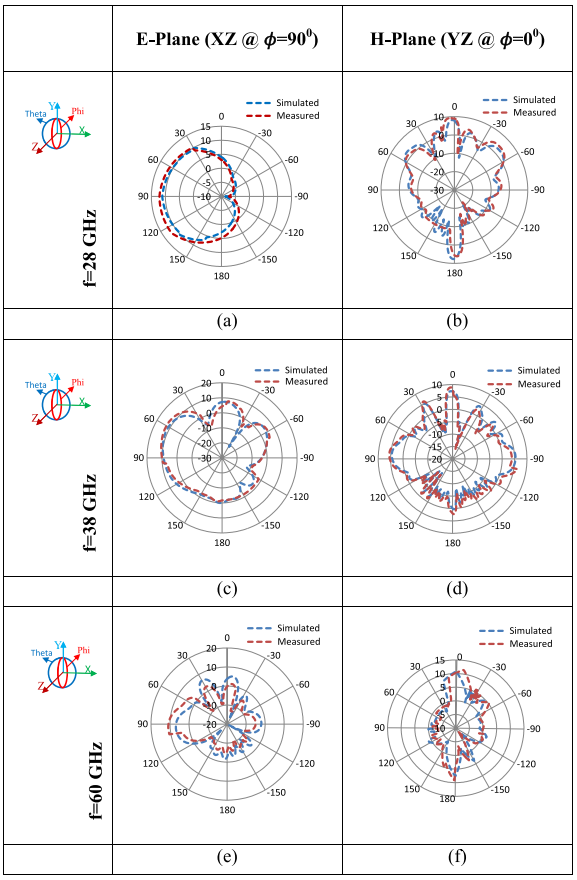


**FIGURE 16.** Comparison of simulated and measured radiation patterns (a) E-Plane (b) H-Plane at 28 GHz, (c) E-Plane (d) H-Plane at 38 GHz, (e) E-Plane (f) H-Plane at 60 GHz.

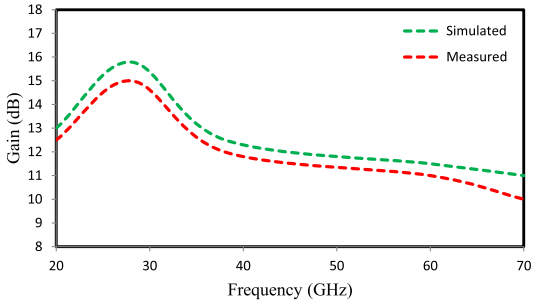


**FIGURE 17.** Comparison of simulated and measured gain verses frequency of eight elements antenna with FSS.

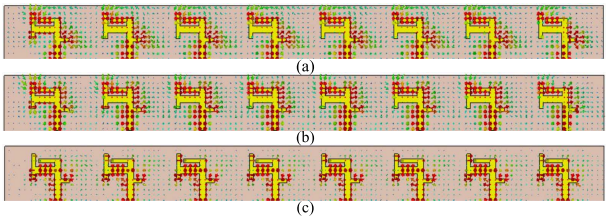


**FIGURE 18.** Surface currents at (a) 28 GHz (b) 38 GHz and (c) 60 GHz.

## V. COMPARISON WITH THE EXISTED DESIGNS

The proposed design is compared to other related antennas with respect to bandwidths, efficiency, operating frequencies,

**TABLE 4. Comparison of proposed 5G antenna with other related antennas.**

| Ref No. | Year | Size ($\lambda\times\lambda\times\lambda$) ($\lambda$ is taken in mm) | Operating Frequency (GHz) | BW (GHz) | Efficiency (%) | Number of elements | Measured Gain (dBi) |
|---|---|---|---|---|---|---|---|
| [30] | 2021 | $2.24 \times 0.14 \times 2.78$ | 28 | 0.85 | – | 1 | 5 |
| [31] | 2021 | $0.94 \times 2.6 \times 0.047$ | 28 | 3.15 | 83 | 4 | 11.65 |
| [32] | 2021 | $0.23 \times 3.17 \times 0.044$ | 28 | 10 | >50 | 8 | 8.1 |
| [33] | 2021 | $0.48 \times 0.48 \times 0.09$ | 28/26 | 5.25 | 85 | 4 | 10.1 |
| [34] | 2021 | $3 \times 0.747 \times 0.115$ | 28 | 4.5 | 80 | 8 | 10 |
| [35] | 2021 | $0.5 \times 0.63 \times 0.09$ | 28 | 6.3 | 88 | 4 | 7.1 |
| [36] | 2021 | $5.2 \times 4.05 \times 0.063$ | 38 | 3.17 | 80 | 4 | 6.25 |
| [37] | 2021 | $1.43 \times 0.67 \times 0.047$ | 28 | 4.7 | 98.6 | 8 | 7.7 |
| [38] | 2020 | $14.57 \times 7 \times 0.09$ | 28 | 5 | 70 | 8 | >8 |
| [39] | 2020 | $14.07 \times 10.28 \times 0.011$ | 28 | 3 | – | 8 | 4–10 |
| [40] | 2020 | $2.33 \times 1.40 \times 0.047$ | 28/38 | 0.9/2 | 84/99 | 1 | 9/5.9 |
| [41] | 2021 | $2\times3.3\times0.05$ | 28/38 | 4.66/7 | >86 | 8 | >10 |
| This work | 2022 | $6.96\times2.5\times0.08$ | 28<br>38<br>60 | 45 | 86<br>87<br>78 | 8 | 15<br>12<br>11 |

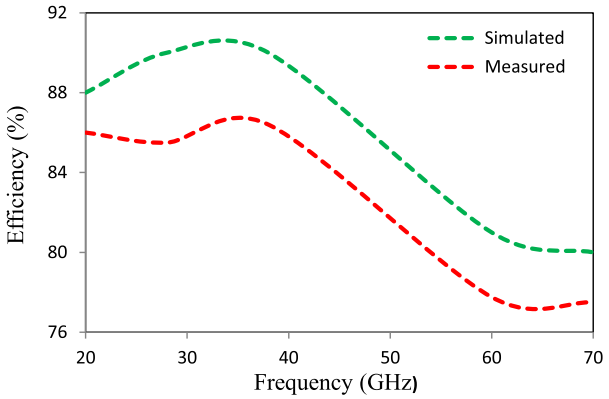


**FIGURE 19. Comparison of simulated and measured radiation efficiency.**

measured gain values, number of elements and size. The size is expressed in wavelength taken in mm at 28 GHz. Comparatively, the proposed design is showing extremely wide bandwidth, better efficiency, higher gain and covering three important bands considered candidate frequencies for 5G communications. A detailed comparison with the related work is shown in Table 4.

## VI. CONCLUSION

In this work, single element antenna with type-A to type-F is designed. The former single element designs were evolved to type-F single element antenna for achieving wide band behavior of the antenna. The proposed antenna system cover a wide range of frequency spectrum from 20 GHz to 65 GHz which covers all candidate frequencies considered for 5G communications. Although, single element type-F has good characteristics like light weight, wide bandwidth, easy to fabricate and stable radiation patterns but it is not preferred for 5G applications due to showing less gain values at the targeted frequencies 28 GHz, 38 GHz and 60 GHz, respectively. The proposed single element is converted into two, four and eight elements, in aiming to achieve the desired gain values for 5G applications. Though gain values were improved at the targeted frequencies with the eight elements antenna design but higher values were obtained by introducing frequency selective surface (FSS). The proposed eight elements antenna with FSS showed good measured gain values 15 dB, 12 dB, and 11 dB at 28 GHz, 38 GHz and 60 GHz, respectively. The proposed design is fabricated and measured results were obtained. A good agreement between simulated and measured results was noted. The proposed eight element array design is considered candidate antenna for 5G applications due to its wider bandwidth, stable radiation patterns, and higher gains at the targeted frequencies.

## REFERENCES

[1] H. Li, M. Wu, Y. Cheng, L. Mei, and C. Zhou, "Leaky-wave antennas as metal rims of mobile handset for mm-wave communications," *IEEE Trans. Antennas Propag.*, vol. 69, no. 7, pp. 4142–4147, Jul. 2021.

[2] J. Bang and J. Choi, "A compact hemispherical beam-coverage phased array antenna unit for 5G mm-wave applications," *IEEE Access*, vol. 8, pp. 139715–139726, 2020, doi: 10.1109/ACCESS.2020.3013068.

[3] A. Li and K.-M. Luk, "Single-layer wideband end-fire dual-polarized antenna array for device-to-device communication in 5G wireless systems," *IEEE Trans. Veh. Technol.*, vol. 69, no. 5, pp. 5142–5150, May 2020.

[4] H. Ozpinar, S. Aksimsek, and N. T. Tokan, "A novel compact, broadband, high gain millimeter-wave antenna for 5G beam steering applications," *IEEE Trans. Veh. Technol.*, vol. 69, no. 3, pp. 2389–2397, Mar. 2020, doi: 10.1109/TVT.2020.2966009.

[5] W. Hong, Z. H. Jiang, C. Yu, D. Hou, H. Wang, C. Guo, Y. L. H. Kuai, Y. Yu, Z. Jiang, Z. Chen, J. Chen, Z. Yu, J. Zhai, N. Zhang, L. Tian, F. Wu, G. Yang, Z.-C. Hao, and J. Y. Zhou, "The role of millimeter-wave technologies in 5G/6G wireless communications," *IEEE J. Microw.*, vol. 1, no. 1, pp. 101–122, Jan. 2021.

[6] M. F. Khajeim, G. Moradi, R. S. Shirazi, S. Zhang, and G. F. Pedersen, "Wideband vertically polarized antenna with endfire radiation for 5G mobile phone applications," *IEEE Antennas Wireless Propag. Lett.*, vol. 19, no. 11, pp. 1948–1952, Nov. 2020, doi: 10.1109/LAWP.2020.3009097.

[7] Y. Q. Guo, Y. M. Pan, S. Y. Zheng, and K. Lu, "A singly-fed dual-band microstrip antenna for microwave and millimeter-wave applications in 5G wireless communication," *IEEE Trans. Veh. Technol.*, vol. 70, no. 6, pp. 5419–5430, Jun. 2021.

[8] Y. He, S. Lv, L. Zhao, G.-L. Huang, X. Chen, and W. Lin, "A compact dual-band and dual-polarized millimeter-wave beam scanning antenna array for 5G mobile terminals," *IEEE Access*, vol. 9, pp. 109042–109052, 2021, doi: 10.1109/ACCESS.2021.3100933.

[9] A. I. Sulyman, A. T. Nassar, M. K. Samimi, G. R. MacCartney, T. S. Rappaport, and A. Alsanie, "Radio propagation path loss models for 5G cellular networks in the 28 GHz and 38 GHz millimeter-wave bands," *IEEE Commun. Mag.*, vol. 52, no. 9, pp. 78–86, Sep. 2014.

[10] W. Hong, K.-H. Baek, and S. Ko, "Millimeter-wave 5G antennas for martphones: Overview and experimental demonstration," *IEEE Trans. Antennas Propag.*, vol. 65, no. 12, pp. 6250–6261, Dec. 2017.

[11] J. Guo, S. Liao, Q. Xue, and S. Xiao, "Planar aperture antenna with high gain and high aperture efficiency for 60-GHz applications," *IEEE Trans. Antennas Propag.*, vol. 65, no. 12, pp. 6262–6273, Dec. 2017.

[12] H. Li, Y. Cheng, and Z. Ling, "Design of distributed and robust millimeter-wave antennas for 5G communication terminals," *IEEE Access*, vol. 8, pp. 133420–133429, 2020.

[13] K. M. Morshed, K. P. Esselle, M. Heimlich, D. Habibi, and I. Ahmad, "Wideband slotted planar inverted-F antenna for millimeter-wave 5G mobile devices," in *Proc. IEEE Region 10 Symp. (TENSYMP)*, May 2016, pp. 194–197.

[14] H. Zhou, "Phased array for millimeter-wave mobile handset," in *Proc. IEEE Antennas Propag. Soc. Int. Symp. (APSURSI)*, Jul. 2014, pp. 933–934.

[15] I. Syrytsin, S. Zhang, G. F. Pedersen, and A. S. Morris, "User-shadowing suppression for 5G mm-wave mobile terminal antennas," *IEEE Trans. Antennas Propag.*, vol. 67, no. 6, pp. 4162–4172, Jun. 2019.

[16] A. Alammouri, J. Mo, B. L. Ng, J. C. Zhang, and J. G. Andrews, "Hand grip impact on 5G mmWave mobile devices," *IEEE Access*, vol. 7, pp. 60532–60544, 2019.

[17] X. Chen, M. Abdullah, Q. Li, J. Li, A. Zhang, and T. Svensson, "Characterizations of mutual coupling effects on switch-based phased array antennas for 5G millimeter-wave mobile communications," *IEEE Access*, vol. 7, pp. 31376–31384, 2019.

[18] I. Syrytsin, S. Zhang, G. F. Pedersen, and Z. Ying, "User effects on the circular polarization of 5G mobile terminal antennas," *IEEE Trans. Antennas Propag.*, vol. 66, no. 9, pp. 4906–4911, Sep. 2018.

[19] M. M. S. Taheri, A. Abdipour, S. Zhang, and G. F. Pedersen, "Integrated millimeter-wave wideband end-fire 5G beam steerable array and low-frequency 4G LTE antenna in mobile terminals," *IEEE Trans. Veh. Technol.*, vol. 68, no. 4, pp. 4042–4046, Apr. 2019.

[20] A. J. A. Al-Gburi, I. B. M. Ibrahim, M. Y. Zeain, and Z. Zakaria, "Compact size and high gain of CPW-fed UWB strawberry artistic shaped printed monopole antennas using FSS single layer reflector," *IEEE Access*, vol. 8, pp. 92697–92707, 2020, doi: 10.1109/ACCESS.2020.2995069.

[21] S. Kundu, "A compact uniplanar ultra-wideband frequency selective surface for antenna gain improvement and ground penetrating radar application," *Int. J. RF Microw. Comput.-Aided Eng.*, vol. 30, no. 10, pp. 1–13, Oct. 2020, doi: 10.1002/mmce.22363.

[22] A. J. Abdullah Al-Gburi, I. B. M. Ibrahim, Z. Zakaria, B. H. Ahmad, N. A. B. Shairi, and M. Y. Zeain, "High gain of UWB planar antenna utilising FSS reflector for UWB applications," *Comput., Mater. Continua*, vol. 70, no. 1, pp. 1419–1436, 2022, doi: 10.32604/cmc.2022.019741.

[23] J. Kim and H. L. Lee, "High gain planar segmented antenna for mmWave phased array applications," *IEEE Trans. Antennas Propag.*, vol. 70, no. 7, pp. 5918–5922, Jul. 2022, doi: 10.1109/TAP.2022.3142333.

[24] J. Puskely, T. Mikulasek, Y. Aslan, A. Roederer, and A. Yarovoy, "5G SIW-based phased antenna array with cosecant-squared shaped pattern," *IEEE Trans. Antennas Propag.*, vol. 70, no. 1, pp. 250–259, Jan. 2022, doi: 10.1109/TAP.2021.3098577.

[25] N. M. Rashad, A. I. Hussein, and A. A. M. Khalaf, "Two-element pharaonic ankh-key array antenna design, simulation, and fabrication for 5G and millimeter-wave broadband applications," *IEEE Access*, vol. 10, pp. 15175–15182, 2022, doi: 10.1109/ACCESS.2022.3148589.

[26] N. O. Parchin, J. Zhang, R. A. Abd-Alhameed, G. F. Pedersen, and S. Zhang, "A planar dual-polarized phased array with broad bandwidth and quasi-endfire radiation for 5G mobile handsets," *IEEE Trans. Antennas Propag.*, vol. 69, no. 10, pp. 6410–6419, Oct. 2021, doi: 10.1109/TAP.2021.3069501.

[27] I.-J. Hwang, J.-I. Oh, H.-W. Jo, K.-S. Kim, J.-W. Yu, and D.-J. Lee, "28 GHz and 38 GHz dual-band vertically stacked dipole antennas on flexible liquid crystal polymer substrates for millimeter-wave 5G cellular handsets," *IEEE Trans. Antennas Propag.*, vol. 70, no. 5, pp. 3223–3236, May 2022, doi: 10.1109/TAP.2021.3137234.

[28] Y. Al-Alem and A. A. Kishk, "Low-cost high-gain superstrate antenna array for 5G applications," *IEEE Antennas Wireless Propag. Lett.*, vol. 19, no. 11, pp. 1920–1923, Nov. 2020, doi: 10.1109/LAWP.2020.2974455.

[29] C. A. Balanis, *Antenna Theory: Analysis and Design*, 3rd ed. Hoboken, NJ, USA: Wiley, May 2005.

[30] Y. Zhang, J.-Y. Deng, D. Sun, J.-Y. Yin, and L.-X. Guo, "Compact slow-wave SIW H-plane horn antenna with increased gain for vehicular millimeter wave communication," *IEEE Trans. Veh. Technol.*, vol. 70, no. 7, pp. 7289–7293, Jul. 2021, doi: 10.1109/TVT.2021.3090096.

[31] U. Ullah, M. Al-Hasan, S. Koziel, and I. B. Mabrouk, "A series inclined slot-fed circularly polarized antenna for 5G 28 GHz applications," *IEEE Antennas Wireless Propag. Lett.*, vol. 20, no. 3, pp. 351–355, Mar. 2021, doi: 10.1109/LAWP.2021.3049901.

[32] J.-Y. Lee, J. Choi, D. Choi, Y. Youn, and W. Hong, "Broadband and wide-angle scanning capability in low-coupled mm-wave phased-arrays incorporating ILA with HIS fabricated on FR-4 PCB," *IEEE Trans. Veh. Technol.*, vol. 70, no. 3, pp. 2076–2088, Mar. 2021, doi: 10.1109/TVT.2021.3061897.

[33] I. L. de Paula, S. Lemey, D. Bosman, Q. V. D. Brande, O. Caytan, J. Lambrecht, M. Cauwe, G. Torfs, and H. Rogier, "Cost-effective high-performance air-filled SIW antenna array for the global 5G 26 GHz and 28 GHz bands," *IEEE Antennas Wireless Propag. Lett.*, vol. 20, no. 2, pp. 194–198, Feb. 2021, doi: 10.1109/LAWP.2020.3044114.

[34] H. Li, Y. Cheng, L. Mei, and L. Guo, "Frame integrated wideband dual-polarized arrays for mm-wave/sub 6-GHz mobile handsets and its user effects," *IEEE Trans. Veh. Technol.*, vol. 69, no. 12, pp. 14330–14340, Dec. 2020.

[35] X.-X. Yang, N.-J. Xie, N.-D. Zhu, G.-Q. He, M. Li, and S. Gao, "Broadband dual-polarized endfire array with compact magneto-electric planar Yagi antenna for mm-wave terminals," *IEEE Access*, vol. 9, pp. 52708–52717, 2021, doi: 10.1109/ACCESS.2021.3068151.

[36] D. A. Sehrai, M. Asif, N. Shoaib, M. Ibrar, S. Jan, M. Alibakhshikenari, A. Lalbakhsh, and E. Limiti, "Compact quad-element high-isolation wideband mimo antenna for millimeter wave applications," *Electronics*, vol. 10, no. 11, pp. 1–10, 2021, doi: 10.3390/electronics10111300.

[37] M. Zada, I. A. Shah, and H. Yoo, "Integration of sub-6-GHz and mm-wave bands with a large frequency ratio for future 5G MIMO applications," *IEEE Access*, vol. 9, pp. 11241–11251, 2021, doi: 10.1109/ACCESS.2021.3051066.

[38] R. M. Moreno, J. Ala-Laurinaho, A. Khripkov, J. Ilvonen, and V. Viikari, "Dual-polarized mm-wave endfire antenna for mobile devices," *IEEE Trans. Antennas Propag.*, vol. 68, no. 8, pp. 5924–5934, Aug. 2020, doi: 10.1109/TAP.2020.2989556.

[39] M. Heino, C. Icheln, J. Haarla, and K. Haneda, "PCB-based design of a beamsteerable array with high-gain antennas and a Rotman lens at 28 GHz," *IEEE Antennas Wireless Propag. Lett.*, vol. 19, no. 10, pp. 1754–1758, Oct. 2020, doi: 10.1109/LAWP.2020.3017129.

[40] P. Liu, X.-W. Zhu, Y. Zhang, X. Wang, C. Yang, and Z. H. Jiang, "Patch antenna loaded with paired shorting pins and H-shaped slot for 28/38 GHz dual-band MIMO applications," *IEEE Access*, vol. 8, pp. 23705–23712, 2020, doi: 10.1109/ACCESS.2020.2964721.

[41] R. Ullah, S. Ullah, F. Faisal, R. Ullah, D.-Y. Choi, A. Ahmad, and B. Kamal, "High-gain vivaldi antenna with wide bandwidth characteristics for 5G mobile and Ku-band radar applications," *Electronics*, vol. 10, no. 6, pp. 1–15, 2021, doi: 10.3390/electronics10060667.

**RAZA ULLAH** was born in Khyber Pakhtunkhwa, Pakistan, in 1992. He received the B.Sc. degree in telecommunication engineering from the University of Engineering and Technology Peshawar, Peshawar, Pakistan, in 2015, and the M.S. degree in telecommunication engineering from the University of Engineering and Technology Peshawar. His research is published in IEEE conferences and peer-reviewed journals. His research interests include designing and analyzing millimeter array antennas for 5G communications, design MIMO antennas, for current and future 5G mobile terminals and MIMO antennas for 5G wireless access points, frequency selective surfaces, EBGs, metamaterial-based antenna, and design of 6G antennas.

**SADIQ ULLAH** (Senior Member, IEEE) received the B.Sc. degree in electrical engineering from the University of Engineering and Technology Peshawar, Peshawar, Pakistan, the M.Sc. degree in electrical engineering from the University of Engineering and Technology Taxila, Pakistan, and the Ph.D. degree for his research in the field of design and measurement of metamaterial-based antennas, in 2010. He is currently a Professor and the Head of the Telecommunication Engineering Department, University of Engineering & Technology Mardan, Mardan, Pakistan. In 2007, he joined the Department of Electronic and Electrical Engineering, Loughborough University, U.K. He worked as an Assistant Manager (Electronics) in a public sector research and development organization in Islamabad, where his main responsibilities were hardware, software co-design, designing and testing of high precession electronics, and test equipment. He has been worked as a Research Associate at Loughborough University, where he researched on the propagation effects of rain, snow, ice, fog, and forest in millimeter wave band. His research is published in international conferences and peer-reviewed journals. His research interests include design and measurement of metasurfaces, metamaterial-based antennas, 5G MIMO antennas, multiband/wideband antenna, SAR, and wearable antennas.

**RIZWAN ULLAH** was born in Khyber Pakhtunkwa, Pakistan, in 1993. He received the B.Sc. degree in telecommunication engineering from the University of Engineering and Technology Peshawar, Pakistan, in 2016, and the M.S. degree in telecommunication engineering from the University of Engineering and Technology Peshawar, Pakistan. He is currently pursuing the Ph.D. degree in telecommunication engineering with the University of Engineering and Technology Mardan, Mardan, Pakistan. His research work is published in IEEE conferences. His research interests include design and analysis MIMO antennas for 4G and 5G smartphone, MIMO antennas for 4G/5G wireless access points, and millimeter wave array antennas for 5G communication.

**IFTIKHAR UD DIN** received the B.Sc. and M.Sc. degrees in telecommunication engineering from the University of Engineering and Technology Peshawar, Peshawar, Pakistan, in 2017 and 2021, respectively. His current research interests include RF Energy harvesting, 5G millimeter wave and MIMO antennas, frequency selective surfaces, EBGs, and metamaterial-based antenna.

**BABAR KAMAL** received the bachelor's degree from BUITEMS, Quetta, in 2012, and the master's degree from the Telecommunication Engineering Department, UET Peshawar, in 2016. He is currently pursuing the Ph.D. degree with the School of Marine Science and Technology, NWPU, China. His research interests include metasurfaces, metamaterials, wearable antennas, multiband/wideband antennas, polarization control devices, and absorbers.

**MUHAMMAD ALTAF HUSSAIN KHAN** received the bachelor's degree from BUITEMS, Quetta, and the master's degree from the Telecommunication Engineering Department, UET Peshawar. His current research interests include RF energy harvesting, 5G millimeter wave and MIMO antennas, frequency selective surfaces, EBGs, and metamaterial-based antenna.

**LADISLAU MATEKOVITS** (Senior Member, IEEE) received the degree in electronic engineering from the Institutul Politehnic din Bucuresti, Bucuresti, Romania, and the Ph.D. degree (Dottorato di Ricerca) in electronic engineering from the Politecnico di Torino, Turin, Italy, in 1992 and 1995, respectively. Since 1995, he has been with the Department of Electronics and Telecommunications, Politecnico di Torino, with a Postdoctoral Fellowship, then as a Research Assistant. He joined the Department of Electronics and Telecommunications as an Assistant Professor, in 2002, and was appointed as a Senior Assistant Professor, in 2005, and as an Associate Professor, in 2014. In February 2017, he was a Full Professor qualification (Italy). In 2005, he was a Visiting Scientist at the Antennas and Scattering Department, FGAN-FHR (now Fraunhofer Institute), Wachtberg, Germany. Since July 2009, he has been a Marie Curie Fellow at Macquarie University, Sydney, NSW, Australia, for two years, where he also held a visiting academic position, in 2013, and in 2014, he has been appointed as a Honorary Fellow. Since 2020, he has been a Honorary Professor with the Polytechnic University of Timisoara, Romania, and an Associate of the Italian National Research Council. He has been appointed as a member of the National Council for the Attestation of University Degrees, Diplomas, and Certificates (CNATDCU), Romania, for the term (2020–2024). His research interests include numerical analysis of printed antennas and in particular development of new, numerically efficient full-wave techniques to analyse large arrays, and active and passive metamaterials for cloaking applications. Material parameter retrieval of these structures by inverse methods and different optimization techniques has also been considered. In the last years, bioelectromagnetic aspects have also been contemplated, as for example design of implantable antennas or development of nano-antennas for example for drug delivery applications. He has published more than 400 articles, including more than 110 journals contributions, and delivered seminars on these topics all around the world: Europe, USA (AFRL/MIT-Boston), Australia, China, and Russia. He has been invited to serve as a Research Grant Assessor for government funding calls (Romania, Italy, Croatia, and Kazakhstan) and as an International Expert in Ph.D. thesis evaluation by several Universities from Australia, India, Pakistan, and Spain. He was a recipient of various awards in international conferences, including the 1998 URSI Young Scientist Award (Thessaloniki, Greece), the Barzilai Award 1998 (Young Scientist Award, granted every two years by the Italian National Electromagnetic Group), and the Best AP2000 Oral Paper on Antennas, ESA-EUREL Millennium Conference on Antennas and Propagation (Davos, Switzerland). He was a recipient of the Motohisa Kanda Award 2018, for the most cited paper of the IEEE TRANSACTIONS ON ELECTROMAGNETIC COMPATIBILITY in the past five years, and more recently, he has been awarded with the 2019 American Romanian Academy of Arts and Sciences (ARA) Medal of Excellence in Science and by the Ad Astra Award 2020, a Senior Researcher, for Excellence in Research. He has been the Assistant Chairperson and the Publication Chairperson of the European Microwave Week 2002 (Milan, Italy), and the General Chair of the 11th International Conference on Body Area Networks (BodyNets) 2016. Since 2010, he has been a member of the Organizing Committee of the International Conference on Electromagnetics in Advanced Applications (ICEAA). He is also a member of the technical program committees of several conferences. He serves as an Associate Editor of IEEE ACCESS, IEEE ANTENNAS AND WIRELESS PROPAGATION LETTERS, and *IET MAP* and a reviewer for different journals.